Article

MAMOTH: An Earth Observational Data-Driven Model for Mosquitoes Abundance Prediction

Argyro Tsantalidou[1,†], Elisavet Parselia[2,†], George Arvanitakis[1,2], Katerina Kyratzi[2], Sandra Gewehr[3], Athina Vakali[1] and Charalampos Kontoes[2]

[1] Informatics School, Aristotle University of Thessaloniki, Thessaloniki, Greece
[2] National Observatory of Athens, IAASARS, BEYOND Center for EO Research and Satellite Remote Sensing, Greece
[3] Ecodevelopment S.A., Thessaloniki, Greece
* Correspondence: tsantali@csd.auth.gr
† These authors contributed equally to this work.

Abstract: Mosquito-Borne Diseases (MBDs) were known to be more prevalent in the tropics, and yet the last two decades they are spreading to many other countries, especially in Europe. The set (volume) of environmental, meteorological and other spatio-temporally variable parameters affecting mosquito abundance makes the modeling and prediction tasks quite challenging. Up to now, mosquito abundance prediction problems were addressed with ad-hoc area-specific and genus-tailored approaches. We propose and develop MAMOTH, a generic and accurate Machine Learning model that predicts mosquito abundances for the upcoming period (the Mean Absolute Error of the predictions do not deviate more than 14%). The designed model relies on satellite Earth Observation and other in-situ geo-spatial data to tackle the problem. MAMOTH is not site- or mosquito genus-dependent, thus it can be easily replicated and applied to multiple cases without any special parametrisation. The model was applied to different mosquito genus and species (*Culex spp.* as potential vectors for West Nile Virus, *Anopheles spp.* for Malaria and *Aedes albopictus* for Zika / Chikungunya / Dengue) and in different areas of interest (Italy, Serbia, France, Germany). The results show that the model performs accurately and consistently for all case studies. Additionally, the evaluation of different cases, with the model using the same principles, provides an opportunity for multi-case and multi-scope comparative studies.

Keywords: Satellite Earth Observation data; Machine Learning; Entomological data; Mosquito-Borne Diseases; Earth Observation for Health; Malaria; Dengue; West Nile Virus;

Citation: Tsantalidou, A.; Parselia, E.; Arvanitakis, G.; Kyratzi, K.; Gewehr, S.; Vakali A.; Kontoes, C. MAMOTH: An Earth Observational Data-Driven Model for Mosquitoes Abundance Prediction. *Remote Sens.* **2021**, *1*, 0. https://doi.org/

Received:
Accepted:
Published:

1. Introduction

Mosquito-Borne Diseases (MBDs) are infectious diseases transmitted by mosquitoes and are responsible for morbidity and mortality in humans. They are part of the Vector-Borne Diseases (VBDs), which account for more than 17% of all infectious diseases and cause more than 700,000 deaths annually [1]. Climate change, travel and trade can influence the seasonal and geographical spread of mosquitoes and thus the transmission of pathogens. Although MDBs can be found in many areas around the world, tropical and subtropical are the ones suffering the most, while different mosquito species carry different pathogens causing various types of MBDs [2]. MBDs, such as West Nile Virus (WNV) transmitted by mosquitoes of the *Culex* genus, Malaria transmitted by mosquitoes of the *Anopheles* genus, and Chikungunya, Dengue and Zika transmitted by *Aedes albopictus* in Europe have posed challenges to national public health authorities in the European region [3].

It is a widely mistaken belief that the MBDs are only affecting the developing countries; Europe has experienced many cases of MBDs outbreaks in the last two decades. 2010 was a year with large outbreaks of West Nile Virus in Greece and Russia, having

262 and 419 human cases respectively and a total of 1016 cases across all Europe [4]. WNV human infections have sharply increased in 2018 compared to the previous years. According to ECDC, in 2019, 615 cases were reported in Italy, 315 cases in Greece, 277 cases in Romania. In total, 1548 cases were locally acquired and 166 deaths were reported. Additionally, 415 WNV cases were recorded in Serbia with 35 deaths [5]. Furthermore, according to ECDC, the number of confirmed Malaria cases reported in the EU from 2008 to 2012 ranged between approximately 5000 and 7000 [6], whereas in 2018 it reached almost 8500 [7]. All the evidence show that there is a need for preventive actions to mitigate the problem.

A lot of earlier research focuses on predicting the upcoming MBDs risk in order to support decision making by successfully designing preventive and mosquito control measures in time and space. The state of the art can be divided into two main directions, one that aims at predicting the upcoming human cases risk (epidemiological approach) and the other that aims at predicting the mosquito populations (entomological approach). As expected, the probability of human infection and the mosquito population in a given area are strongly dependent variables [8].

A number of issues have posed difficulties in mosquito population monitoring and forecasting up to date. The lack of well structured, consistent and reliable environmental, landscape and ecosystem data, and their change over time that makes them hard to collect, are some of the most important barriers. The necessary placement of in-situ equipment for environmental data collection is limiting the study area either because of the high cost of operation and maintenance or the inaccessibility of an area. Different spatio-temporal resolutions, re-sampling and filtering techniques in limited areas increase significantly the complexity of comparative studies. However, the advent and plethora of satellite Earth Observation (EO) Big Data from multiple sensors (e.g. Sentinel, Landsat, TERRA/AQUA (MODIS), etc.), which allow frequent revisit times and larger coverage, enable enhanced earth monitoring at global level and provide vast amounts of data that are consistent and accessible via open data platforms [9]. In addition, the revolution in data science and machine learning (*ML*) algorithms provides many opportunities for accurate and reliable data-driven solutions to the problem [10].

Related work

There are approaches that evaluate analytical dynamic models to predict the upcoming human infections or the mosquito populations. In [11], researchers attempted to identify conditions conducive to a WNV outbreak in Greece using an epidemiological model of differential equations. Other approaches use environmental/meteorological data and simple statistical approaches that attempt to identify the conditions favoring the spread of MBDs and can be used for mitigation measures. Authors in [12] concluded through observational analysis that a rapid increase in temperature is associated with an increase in human WNV cases in the West Virginia area of the United States. Authors in [13] perform a two step cluster analysis to classify areas in Greece into low, medium and high risk for the spread of WNV virus. In [14], a statistical analysis was performed for Morocco and it was found that extreme rainfall and high Normalized Difference Vegetation Index (NDVI) values are the factors that contribute to WNV amplification.

In recent years due to the progress in the field of ML a lot of valuable studies that combine remote sensing data with ML techniques have been proposed. The authors in [15] proposed a novel machine learning method for classification of high-spectral images based on the estimated spectral profiles per pixel, providing a promising segmentation of materials lying over or beneath the Earth's surface, while the authors in [16] proposed the use of deep learning classifiers which combine different sources of information and extract high level features, able to achieve better classification results with remote sensing images. More detailed information can be found in [17]. This overall progress in the field of remote sensing offered more sophisticated data-driven models to help control MBDs. A lot of algorithms have been used in different areas with various features and techniques. [18] and [19] used Support Vector Machine (SVM) to predict Malaria and Dengue cases in India and China respectively. Both were based on epidemiological and environmental data. General additive models are also a popular method for predicting WNV in the Great Plains of the United States [20] and Malaria in Kenya [21]. The K-Nearest Neighbors (KNN) algorithm was utilized to estimate the weekly mosquito population in northwestern Argentina [22]. Authors in [23], after training many decision trees to predict WNV incidence across different areas of the United States over the years, concluded that there is not a single model fitting one area over the years, but rather a model fitting many areas in a specific year is more feasible.

However, in all cases studied, limited selected environmental data were included, such as temperature and precipitation, which were used as predictors along with other kinds of features depending on each case study. Each work presents a model or an architecture that focuses on a specific mosquito genus/disease and area of interest, so all of these approaches are not directly comparable and are site specific and genus specific. These limitations hinder the scalability and generic applicability of the developed approaches. In this view arises the need for a generic integrated, scalable and reliable Early Warning System (EWS). The idea of the prototype EYWA system, developed under the flag of the EuroGEO Action Group for Epidemics, came to overcome several of the above mentioned limitations, thus delivering a scalable and robust solution as shown in the following sections.

Our approach

This work is motivated by the lack of a widely accepted, standardized and generic solution for the problem of mosquito abundance predictions. Taking advantage of the recent progress in the ML domain, and integrating multi-source EO data to extract environmental, landscape and ecosystem related information in a consistent, uniform, and reliable way, we focus on designing an early warning predictor of the upcoming mosquito population. Our goal is to design a location and genus agnostic model out of a generic and adaptive framework. This gave birth to MAMOTH (Mosquitoes Abundance Prediction Model autO-calibrated from features pleTHora), presented hereinafter, a generic framework that requires no human intervention in selection of the features or model's hyper-parameters tuning. In this paper we present the application of MAMOTH in 5 different use cases, comprising of different combinations of mosquito species and Areas of Interest (AOI). Our cases include three different mosquito species and four different areas. From our study cases, a comparison of the same mosquito (Culex pipiens) in three different areas can be performed, as well as a comparison between two different mosquito species in the same AOI. Initially the framework was applied for mosquitoes of the Culex genus in the Region of Veneto in Italy. The performance analysis showed that the accuracy results are promising, consistent with respect to the month of the prediction and robust against sensitive features. All the aforementioned predictions took place on the trap site, but this is not mandatory. As we saw on the results, the performance is promising even without using past entomological features for the prediction.

After the exploration of the initial case (Culex genus mosquitoes in Veneto region of Italy), the framework has been applied to extra four use cases such as Anopheles spp. also in the Veneto Region of Italy, Culex pipiens in the Vojvodina region of Serbia, Culex pipiens in the Baden Wuerttemberg region of Germany and Aedes Albopictus in Grand-Est and Corsica regions of France and the results verified that the performance is consistent among different cases. In a nutshell, our work contributions are summarized in its capacity to offer:

- **Design an auto-calibrated mosquito forecasting model**: that combines Earth Observational and entomological information. Our approach allows for a generic framework that wraps itself around each case through automated feature selection and hyper parameters tuning process. This approach of feature selection prevents the injection of human bias into the model, while allowing for further analysis on the selected feature set. Framework's description is presented in Section 3.

- **Accurate robust forecasting model, tested in actual measurements**: for mosquito populations, independently of location and genus contextual constraints. The ML approach followed in combination with the automated selection of features enabled for an auto adjusted and accurate framework validated upon five different cases (consisting of 4 different areas of interest and 3 different mosquito species), with different contextual constraints delivering high performance presented in Section 4.
- **Comparative study**: due to the replicability of our framework that uses the same architecture and the same mathematical principles offers the extensive capability of comparative studies among different cases, responding to: "which characteristics seem important in one case and which in another?" as we can see in the comparative study of Section 4.

To the author's knowledge, this is the first time that a single data-driven architecture has predicted mosquito populations of different species in a way that tackles several MBDs simultaneously and is independent to the site of application thus presenting a high rate of transferability in different landscapes and climatic zones.

In the remaining parts, the paper is organized as follows, Section 2 presents the collection, augmentation and prepossessing of the entomological and EO data. In Section 3 a detailed description of the entire architecture with all the corresponding self-learning modules is given. Section 4 presents the case studies in which the system was applied and the corresponding performance is reported and analyzed. Section 5 is a discussion of the results and the next research steps.

2. Datasets

This section, presents the components of the preparation of the dataset. Includes the collection of the Earth Observation and the entomological data, as well as, their preparation to be used from the ML algorithms.

Open EO Data

The predictive model uses environmental variables (geographical, climatic, and hydrological) that influence the transmission cycle between pathogens, vectors and hosts.

This study used remote sensing indices that have shown strong correlation with mosquito behaviour and biological cycle. To compute the satellite derived Normalized Indices, a number of the satellite's band were used, namely the Near Infrared (NIR), the Red (RED), the Short Wave Infrared (SWIR) and the Green (GREEN) band as shown in formulas (1) - (4). The Normalized Difference Vegetation Index (1) (NDVI), the Normalized Difference Water Index (2) (NDWI), the Normalized Difference Moisture index (3) (NDMI), and the Normalized Difference Build-up Index (4) (NDBI) are used as proxies for vegetation density, changes in vegetation water content, determination of vegetation water content and mapping of built-up areas respectively. To quantify these environmental indicators for the period from 2010 to 2020, the satellite images Sentinel 2 (10m GSD, 6-days revisit time) and Landsat TM 7 & 8 (30m GSD 16-day repeat cycle) were accessed and pre-processed. The images were resampled to a uniform grid of 500m x 500m to obtain a spatially harmonized dataset.

$$NDVI = \frac{(NIR - RED)}{(NIR + RED)} \tag{1}$$

$$NDWI = \frac{(GREEN - NIR)}{(GREEN + NIR)} \tag{2}$$

$$NDMI = \frac{(NIR - SWIR)}{(NIR + SWIR)} \tag{3}$$

$$NDBI = \frac{(SWIR - NIR)}{(SWIR + NIR)} \tag{4}$$

Temperature affects several processes associated with the mosquito as well as the rate of virus development within the vector is associated with warmer temperatures [24]. The MODIS sensor from TERRA & AQUA was used to estimate Land Surface Temperature (LST), which is estimated from top-of-atmosphere brightness temperatures from the infrared bands of the satellite's sensors. The product incorporated into the model is the V6.0, which provides daily LST daytime and nighttime values and emissivity with a spatial resolution of 1 kilometer (km).

Precipitation can have both, a positive effect on the larval carrying capacity of breeding sites and a negative effect on the mosquito reproductive cycle interrupting it by flushing away aquatic stages from container breeding sites. [25]. The Integrated Multi-satellitE Retrievals for GPM (IMERG) precipitation grid with a resolution of 0.1° x 0.1° was used to extract the daily precipitation on the day each trap was placed. The accumulated rainfall values for one week, two weeks before each trap's date of placement as well as accumulated rainfall from the 1st of January of each year were also calculated.

Meteorological Data

High wind speed is correlated with lower abundances of infected mosquitoes in traps. It seems that in high wind speed situations the reduced flying and biting activity of mosquitoes lead to lower transmission rates of WNV [26]. The ERA-5 Land Search Results Numerical Weather Prediction product was used with a native spatial resolution of 0.1° x 0.1° (hourly u and v components at 10m). Further processing resulted in retrieving the hourly wind components from the relevant GRIB ERA5-Land file at the point-date level and calculating the daily min, max and mean values including the dominant wind direction.

Auxiliary data

Topography has been indicated as a significant factor in the transmission of MBDs, while it also influences the biotic conditions of different mosquito species and indicates the most suitable breeding sites. The Digital Elevation Model (DEM) product used to generate parameters such as elevation, slope and aspect was acquired from Copernicus LMS with a spatial resolution of 25 meters. For each point (trap station, WNV reported human case, village), the mean elevation, slope and aspect were calculated within a buffer zone of 1 km around the point. The buffer radius was determined based on the flight range of the Culex spp. [27].

The challenge of processing big time series satellite data from different sensors at EU level and generating the relevant indices for the last 10 years was addressed by using the cloud-based geospatial processing platforms CREODIAS and Google Earth Engine (GEE). CREODIAS has been adapted to process big EO data, including a EO data storage cluster that allows live access to the entire Sentinel data collection at any time, without the need to submit a job to Cloud Archive and wait for it to become available. In turn, GEE is another big EO data analysis platform that has been used complementarily for the collection and processing of Landsat TM 7 & 8 and MOD11A1 V6 imagery by taking full advantage of the open source API Earth Engine Python and Earth Engine Catalog, enabling for fast computations.

Remote sensing data preparation

The multi-spectral satellite data obtained from various sensors with different spatial and temporal resolutions had to undergo spatial and temporal integration. The higher resolution satellite sensors have been pre-processed and spatially resampled to 500m by aggregating the information of the native pixel resolution of 30m GSD in case of Landsat TM 7 & 8 and 10m GSD in case of Sentinel 2. The MODIS the native spatial resolution of 1 km was resampled to 500m by splitting the pixel into 4 equal value pixels. To deal with the diverse revisit time of the satellites, the data have been temporally resampled following the every other week circle of the entomological collection, by choosing the last available record. Since the EO data used were optical, we had to set a time threshold for the last available record for missing values due to cloud coverage. Therefore, the time window to search for the last available value has been set to one week for the LST and to one month for the indices. If no data were found during this time window, the value was assigned as missing value. For each of the in total 19000 in-situ observations that were distributed in 4 countries, 21 EO variables were computed (see Table 6 in appendix for a detailed description of features). The term observation refers to one in-situ trap observation within a single time stamp. The EO variables were retrieved by processing big data with the volume of the satellite imagery approaching 200Tb.

Entomological Network

A systematic approach for entomological monitoring has been effective since 2010 for Europe, collecting data from stable station networks. The entomological surveillance of the AOI in this work has made use of CDC-CO2 light traps and gravid traps, collecting mosquitoes each year on roughly every other week basis, identifying the total number of mosquitoes and the number of mosquitoes tested positive to the pathogen. As an example Figure 1 depicts the entomological network in the Veneto region of Italy.

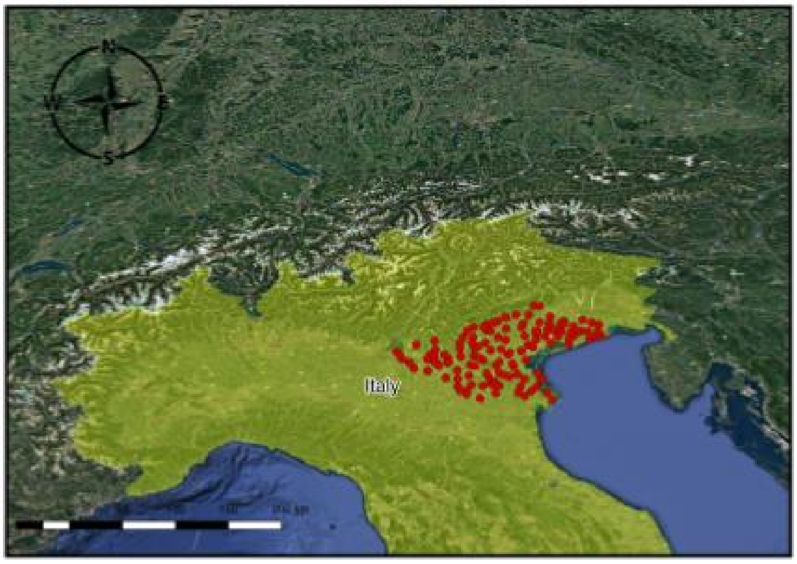

Figure 1. Veneto region in Northeast Italy (Top Left 10.62, 45.81 Bottom right 13.08, 44.94, Datum WGS84). The entomological monitoring network of 140 traps of the Culex pipiens in the Veneto region.

Data pre-processing

Final datasets, formed after the integration of multi source data, suffered from inconsistencies / erroneous insertions that had to be tackled. Duplicates of records were removed, while missing values in the dataset were filled using the method of iterative imputation, by modelling each feature with missing values as a function of other features in a round-robin fashion [28].

The range of several features varies a lot, which may be a problem when used with ML algorithms. The variance of the features with greater magnitude might contribute that much on the cost function and vanish the features with smaller magnitude. So a normalization from -1 to 1 was applied to the indexers, to ensure that all indexers will be treated equally from the learner.

3. MAMOTH Principles and Methodology

In the usual supervised ML setting, we assume an initial dataset X consisting of a number of observations (rows) and a number of features (columns) called the feature-space. Additionally, each observation corresponds to a label/target variable y that should be estimated $\hat{y}$ from the ML model $f(\cdot)$ by observing the input information X and a set of learnable parameters ϑ,

$$f(X|\vartheta) = \hat{y} \ . \tag{5}$$

In our case, X is the set of EO and entomological features that we know, θ are the internal parameters of the model and $\hat{y}$ is the prediction about the mosquito abundance for the upcoming period. The goal of the ML algorithm is to find, through the training process the optimal learnable parameters ϑ of the model that minimize the cost between the real target of each observation and the corresponding estimated one. The aforementioned approach raises three fundamental modeling questions that should be specified: i) Cost function - What do we aim to solve? ii) Feature space selection - Which representation of the input is suitable for the optimization process? iii) Solver - How are we going to solve the optimisation problem?

In this section, we present MAMOTH, a framework for Mosquitoes Abundance Prediction Model, by answering the above modeling questions. As mentioned (see introduction section), MAMOTH main characteristic is that the user does not have to specify the feature space of the observations or models hyper-parameters. Instead, an auto-calibrated model is created based on the proposed architecture described in Figure 2 that receives the initial dataset and self-tunes its hyper-parameters. It decides which features to use build a custom prediction model that is meaningful for the AOI each time.

MAMOTH's Cost function

We transform mosquitoes' populations from a regression to an ordinal classification problem, that offers multiple advantages both in the technical domain and in disseminating the results to a non-technical audience. Technically, this transformation makes our model more robust to outliers since the contribution of a single observation's error is limited. In terms of dissemination, it helps a non-technical audience to understand the results e.g. "In the next two weeks the model expects a mosquito abundance class 8 out of 10 for this region", is more informative compared to "In the next two weeks, the model predicts an average of 183 Culex mosquitoes for this region".

Accordingly, the cost function aims to minimize the Mean Absolute Error (MAE) between the real and predicted mosquito abundance classes.

$$MAE = \frac{1}{n}\sum_{i=1}^{n}|y_i - \hat{y}_i| \ . \tag{6}$$

It is worth mentioning that the results obtained with MAE criterion (and being presented in Section 4), are similar to the results obtained with the mean square error criterion for the cases studied so far. Due to the analytical properties of the mean square error criterion, the training of the model is computationally much lighter than with mean absolute error criterion, so it can be used when we need a fast re-training of the models.

MAMOTH's Feature space and solver

From the initial feature space as described in Section 2, MAMOTH automatically decides on the proper number of features and the features themselves for every specific case (different mosquito species or different area). The solver of the model is relying on Gradient Boosting ML technique for regression. Gradient Boosting machines belong to a very powerful and popular family of ensemble techniques that combine numerous weak learners in order to produce a powerful learner [29]. The parameters that have to be tuned are the max depth of the trees constructed and the number of estimators (number of trees) since our gradient boosting model relies on decision trees. Regarding the purpose of the parameters, the tree depth indicates the complexity capabilities of the algorithm, and the number of estimators refers to the quantity of estimators that will be used with the sequent estimator correcting the previous one. The hyper-parameters of the solver, as well as the selection of the feature space are automatically specified by MAMOTH as illustrated in the pipeline of Figure 2.

Description of MAMOTH's pipeline: As depicted in Figure 2 the model's architecture consisted of 5 main modules i) Feature Expansion / Engineering ii) Pre-process iii) Parameters Grid iv) Feature Selection v) Model Selection. The main advantage of this architecture is that even if the final model is complex, each module, separately, is simple and its functionality is quite intuitive. This advantage is crucial for the implementation and the further evolution of the model.

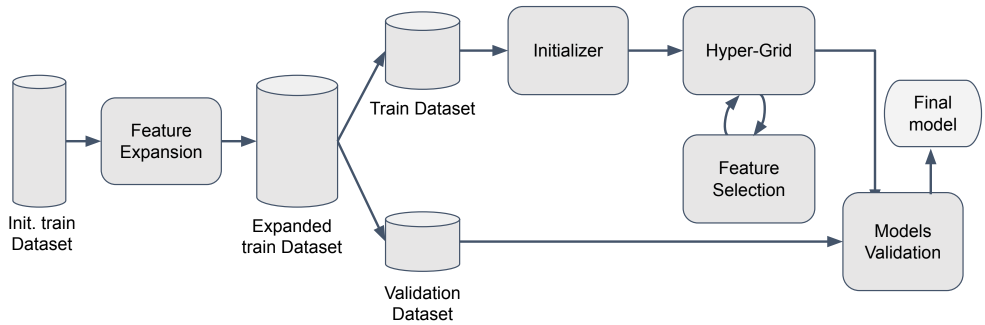

Figure 2. MAMOTH Pipeline Outline

Feature extraction / engineering Module

The information that is already included in the dataset can be used/restructured to generate new features that are informative regarding the target variable in a more algorithm-friendly way. This process requires a strong understanding of the physical problem and a good knowledge of the related work to guide the selection of valuable features for the ML algorithms. This process involves various operations on the feature space, such as i) non-linear transformations, ii) linear and non-linear combinations, iii) temporal and spatial shifts, iv) moving averages, v) variables related to spatial clustering of the data, vi) strong components of PCA, vii) thresholds for variables. The goal is to provide a more extended pool of features to the next modules. Respecting the trade-off between information and complexity leads us to the most limited number of features that capture spatial and temporal information that could be useful for prediction. At this point it should be stated that removing this module out of the framework's pipeline is possible, but based on our experiments this led to an average 20% decrease in the performance. The features used in this paper can be found in the Appendix in Table 6.

Initialisation Module

This module obtains as input the training set and starts the initialization of the training process i) Determine the mosquito abundance classes: Calculate the range of each abundance class and perform balance handling if needed. The range of each class is selected so that all classes have equal probability of selection. In this paper, the number of mosquito abundance classes is set to 10 ii) Target set: the optimal time distance for prediction according to the training set is selected or proposed to the user, e.g., predict the mosquito abundance for the next 15 days or 30 days. To determine the optimal time distance for the target set, a CDF (Cumulative Distribution Function) of the time distance of days between two consecutive observations was created and the minimum time distance that covers as much of the dataset as possible is selected. iii) Initial tuning: uses the most correlated features (according to Pearson correlation score) to make an initial rough estimate on the hyper-parameters of the model in a gradient-based manner (max_depth, number of estimators).

Hyper-parameters Grid Module

It takes as input the initial estimate of the model's hyper-parameters and generates parameters' grid points around these values. For each of these points, the Feature Selection module outputs a single model. This stage is useful for further fine-tuning the model's hyper-parameters. This module improves the overall performance of the model, but we should mention that in most of our experiments this improvement was less than 7%. So, in case of limited computational resources, we can skip this module and build a mode directly in the initial estimation of the hyper-parameters of Initialisation Module.

Features Selection

For each point in the parameters' grid, the system starts with the entire set of features, as specified in the feature extraction/engineering module, and uses recursive feature elimination and cross-validated selection to select both the optimal number of features in the feature space and the features themselves. In the feature elimination, the ranking of each feature is done according to the usual relative importance score [30]. Finally, we use the coefficient of determination, known as R^2 score, in a 10-fold cross-validation set to select the model with the optimal number of features. This process slightly increases the complexity of the model (k-fold cross-validation is a linear operation in terms of resources) but makes the model more robust to randomness and bias.

Model Selection

Finally, each model of the grid point is evaluated with unseen validation data, and the final model is selected according to the mean absolute error criterion (optionally, this criterion can be changed to the mean squared error).

The model's predictions are assessed using the same metric as the cost function used during the training phase, the MAE. This metric indicates the distance between the actual class and the predicted class, which gives a simple intuition of the quality of the prediction. Another metric that can characterise the quality of the system is the percentage of predictions with an error equal to or less than 3 classes. This metric quantifies the percentage of the time that the predictions do not deviate too much.

Computational cost

A fundamental aspect of a machine learning model is the computational cost (complexity). Our framework uses a Gradient Boosting model as learner, so, is directly affected by decision tree cost which is equal to $\mathcal{O}(mnd)$ [31], where n is the number of observations in the training set, m is the number of features and d is the depth of the tree. Since Gradient Boosting Models construct M different decision trees the model's computational cost is $\mathcal{O}(M(mnd))$. The framework applies a greedy search for optimal features by training multiple gradient boosting models and recursively eliminating the least significant feature, this increases linearly the overall complexity with respect to the number of features to $\mathcal{O}(M(m^2nd))$. So the more the features available, the more gradient boosting models will be constructed, and thus the higher the overall computational cost will be. Hyper-parameters grid module can also add in computational cost due to the repetition of the above mentioned process, as it executes exhaustive search in a window (e.g. of 5×5) around the initial hyper-parameters estimation (max_depth,number of estimators), this module multiplies the overall computational cost by a factor equal with the number of grid points (e.g. 25). It can be concluded that MAMOTH's computational cost is affected quadratic by the number of features m used and linearly by the hyper-parameters tuning grid.

4. Experimentation

In the Experimentation section we present the application of our framework to a total 5 different cases (three different mosquito species and four different areas). The cases cover scenarios that allow us to perform comparative analysis, such as the same mosquito species (Culex pipiens) in three different areas or two different mosquitoes species in the same area of interest.

We applied MAMOTH to the Veneto region in Italy to predict the population of Culex pipiens. These predictions took place on the trap site, since the model uses the historical entomological data as input features in the training process. The models' performance was also tested for off-trap-site predictions with promising results, in this experiment the training of the model did not use past entomological information as input features.

The validation of the framework was conducted in 2 different ways, *operationally* on last year's data and *pre-operationally*. Operational validation is designed to imitate the real life conditions and pre-operationally validation operates on multiple random realisations (via *k*-fold validation) to verify that the received performance is not an outlier. More specifically on the *Operational* validation we test separately each month of 2020. When testing on a specific month's data, the rest of the data past this month will be completely ignored by the training process as they belong to the future and we know nothing about them. This process goes on iteratively to cover all available months of last year's data. For example, if we want to predict the abundance of mosquitoes in July of 2020, observations until July of 2020 will be used as training set, while observations past July will be completely ignored. This method was applied iteratively in a cross validation fashion to assess the model's performance. *Pre-operational* validation is a classical 10-Fold cross validation method where all observations are taken into account without any time constraints. This process rules out any performance inconsistency due to a specific time series behavior and verifies that the results of the operational validation is not an outlier. Results showed that the two kinds of validations perform similarly, with pre-operational validation achieving slightly better results as expected. Also, we conducted experiments for a comparative study and we applied the framework in Vojvodina (Serbia) and Baden Wuerttemberg (Germany) to further test its performance for the abundance of Culex mosquitoes. We also extended the model to two other species, Anopheles spp. in Veneto (Italy) and Aedes albopictus in Grand-Est and Corsica (France). In all these cases, the results were promising and consistent.

Area of interest and Entomological network

The study area is located in Northeast Italy, at the Veneto region as depicted in Figure 1. The area includes the eastern part of the Alps and the northeastern part of the Po Valley. The average temperature during the period of interest had a mean value of 25.4 degrees Celsius and the cumulative precipitation has been 30mm.

The entomological monitoring of Culex pipiens in the Veneto region has been effective from 2010 to 2020, gathering data from a network of 140 stations and resulting in a dataset of more than 4800 observations.

Table 1 presents class separation of the initialization module, the corresponding number of mosquitoes for each class as well as the probability of having at least one mosquito positive to WNV. It can be observed by Table 1 that the probability is monotonically increasing as the number of mosquitoes increases, which supports the claim that the higher the mosquito population the higher the WNV circulation and thus its dissemination in the community.

In case of Culex mosquitoes in Italy nearly 80% of the observations had at most a 15 days time distance between two consecutive observations of the same stations as shown in Figure 3. So the target of prediction was set to 15 days to keep as many observations as possible while keeping a reasonable prediction time in order to grant authorities time to take preventive actions against mosquitoes if needed.

Table 1: Culex Mosquito Risk Classes

<table>
<tr><th>Class</th><th>Number of mosquitoes</th><th>Probability of at least one mosquito positive to WNV</th><th>Risk class</th></tr>
<tr><td>1</td><td>0 - 3</td><td rowspan="2">0.23 %</td><td rowspan="2">low</td></tr>
<tr><td>2</td><td>4 - 9</td></tr>
<tr><td>3</td><td>10 - 18</td><td rowspan="2">1.07 %</td><td rowspan="4">medium</td></tr>
<tr><td>4</td><td>19 - 34</td></tr>
<tr><td>5</td><td>35 - 58</td><td rowspan="2">2.82 %</td></tr>
<tr><td>6</td><td>59 - 100</td></tr>
<tr><td>7</td><td>101 - 167</td><td rowspan="2">6.35 %</td><td rowspan="4">high</td></tr>
<tr><td>8</td><td>168 - 293</td></tr>
<tr><td>9</td><td>294 - 568</td><td rowspan="2">8.01 %</td></tr>
<tr><td>10</td><td>> 568</td></tr>
</table>

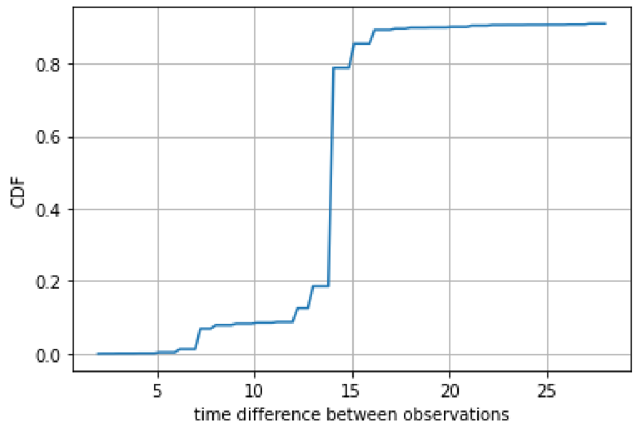

Figure 3. CDF of time difference in days between 2 consecutive observations for the case of Culex Italy

Furthermore, the auto-calibration process was tuned to max_depth = 5, number of estimators = 23 and decided that the optimal number of features is 16. The selected features with their corresponding importance are presented in Figure 4.

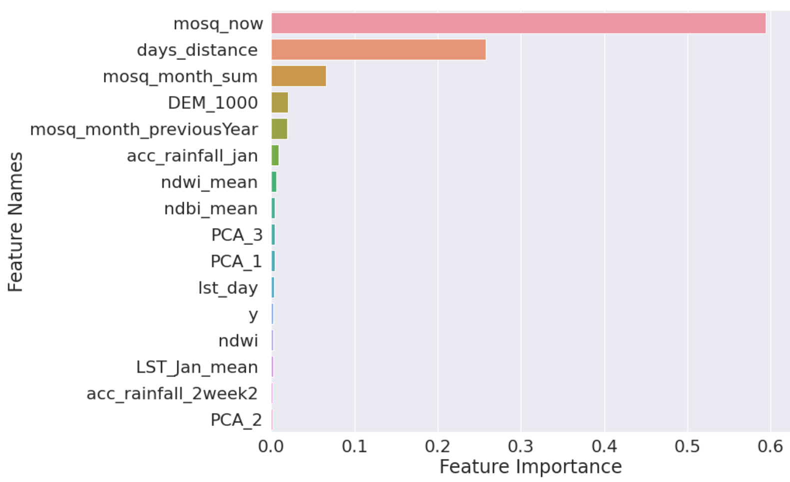

Figure 4. Feature Importance of Culex Italy case using both EO and entomological data

It is clear that the most important feature which affects mainly the prediction of mosquito abundance class, is the current mosquito population. Additionally, the accumulated mosquito populations of the running month seems to play an important role in the formation of the final prediction. Those two features are capturing the temporality in an indirect way, the current state is very important for the upcoming state, and seems to be important in all Culex mosquito cases independent of the area of interest. Temporality is directly captured by the days distance from a certain date regardless of the year, indicating that the mosquito population is partly following a pattern. Besides the temporality and mosquito population though, presence of water is also a considerable factor as measurements on its different states are selected by the system by 3 different features (NDWI, two past weeks cumulative rainfall and cumulative from January rainfall). Temperature is also selected and represented by 2 features, however affecting much lower in the final prediction than expected based on relevant literature which claims that temperature is one of the main contributor for the mosquito population. Spatiality expressed by the latitude and elevation of the trap site are also features that the system chose to make more accurate predictions.

Culex Veneto Results

The MAE for all the predictions is 1.27. The error distribution in Figure 5 shows that most of the errors are spread across a small range, meaning that 97% of the predictions are less or equal to 3 classes away from the actual class. Those promising results shows that the system's predictions are most of the time very close to the actual mosquito population that we aim to predict.

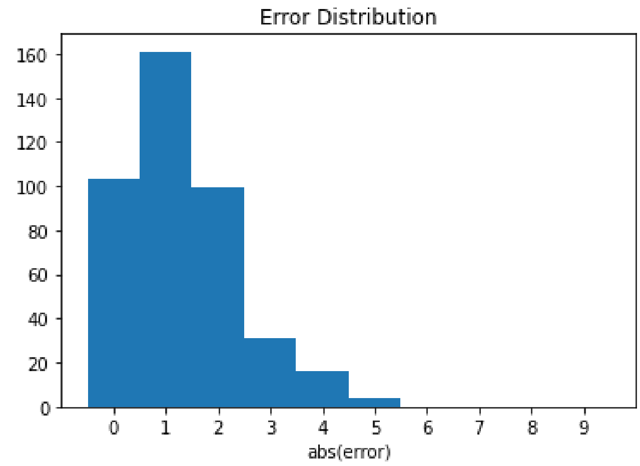

Figure 5. Error Distribution of Culex Italy case using both EO and entomological data

Error distribution among risk classes

In the plot of error of each class in Figure 6, we can see that the model is performing similarly in all mosquito abundance classes, without any strong bias to low or to high abundance classes.

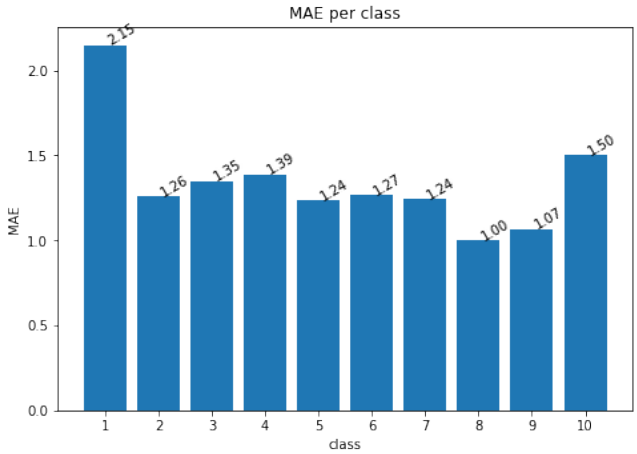

Figure 6. MAE per class of Culex Italy case using both EO and entomological data

Results per month

The prediction error of each month is relatively equal, the MAE in June is higher due to smaller size of dataset and the lack of data, before May of 2020, thus training the model only upon data of previous years and not in recent observations. Respectively, the MAE of October is lower than the others, due to the training of the model in many more recent observations.

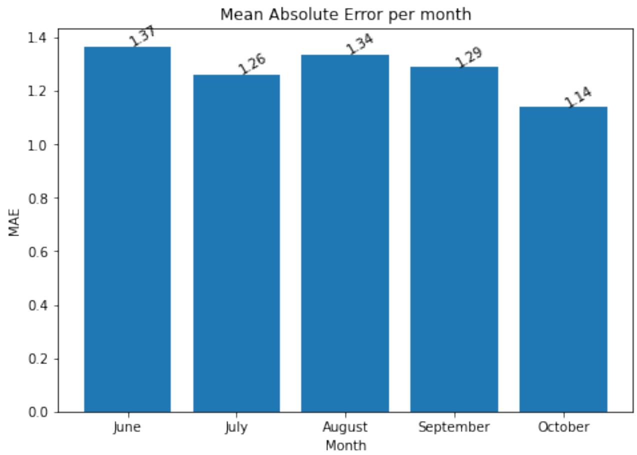

Figure 7. MAE per month of Culex Italy case using both EO and entomological data

To validate the performance of the model except the operational application, the system was tested on random 10-fold validation using all the available data. The results showed slightly better behavior, in terms of MAE: 1.14, and similar performance in terms of percentage of error below 3 classes: 97%. This slight improvement can be explained by the fact that in the k-fold validation the samples for train and test process are selected uniformly from the entire dataset compared to the operational case where train and the test sets are totally separated in time. Those results are leading us to the conclusion that the performance of the model is stable according to train-test separation of the dataset.

Performance without the Entomological features

As depicted in Figure 4 the model relies a lot on the entomological features in order to predict the mosquito population for the upcoming period. The current number of Culex mosquitoes is the *most important* feature by far, while also the feature with the *third highest* relative importance score being the sum of Culex mosquitoes of the past 30 days and the *fifth highest* feature on the list is the mosquito population of the same month the previous year. The need of those entomological features could limit the wide use of the model, once this information is known only on the trap-site. Away of the trap-sites this information will not been known. Thus, the question that we like to answer is, could the model perform reliably if those important entomological features are missing from the feature space?

To test this hypothesis we removed all features relevant to entomological data and we re-training a new MAMOTH model using only EO data and features derived from them. The results showed that the model was still able to accurately predict the upcoming mosquito population with a small accuracy reduction compared to the model that used entomological features. The new MAMOTH model performed with 1.65 MAE and the percentage of errors below 3 classes was reduced to 92%. The wide applicability of a model that relies only on EO data, marks those results as promising for further research in that direction.

As seen in Figure 8, the new model in order to fill the gap that was created by the absence of the entomological features, increased the total amount of selected features to 34 (compared to 16 of the model with the entomological features), along with the significantly increased importance of EO related features such as rainfall, LST, NDWI, NDVI, NDBI.

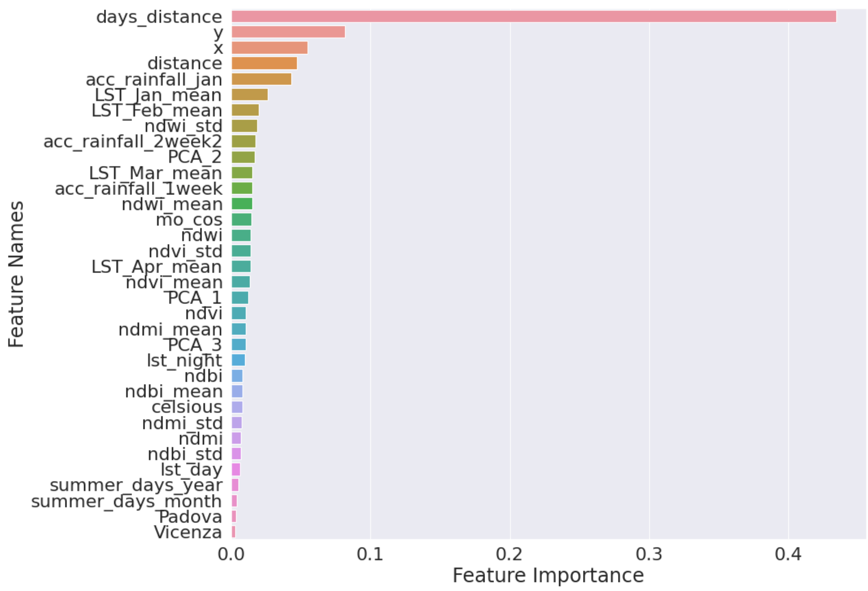

Figure 8. Feature importance of Culex Italy case using only EO data

Performance without the EO features

As mentioned above, even in lack of entomological data, MAMOTH was still able to predict the upcoming mosquito abundance using only EO data and features derived by them. However, for the sake of completeness, it is of great importance to investigate the performance of the framework without using any EO data. To test the performance of the framework without the presence of EO data, we removed all the related EO features. The results showed that the performance of the model was a slightly decreased comparing to the previous case where EO and entomological data were available. More specifically the error climbed up to 1.34 and the percentage of errors below 3 classes was reduced to 94% using 15 features.

As we can see in Figure 9 the model basically relies on the current mosquito population and the seasonality of the observation in order to deliver accurate predictions. This version of the model points out the significance of the entomological data, as without any EO information available the performance of the model was not deviating much from the initial model with EO and entomological information available. However, even in lack of them, a similar result can be achieved using only EO data.

Table 2: Final data-set of each case

Area of interest - Mosquito	Year	# of traps	# of observations
Italy - Culex pipiens	2010 - 2020	140	4840
Serbia - Culex pipiens	2010 - 2019	124	926
Germany - Culex pipiens	2010 - 2019	86	3763
France - Aedes Albopictus	2017 - 2019	81	1729
Italy - Anopheles spp.	2010 - 2020	130	629

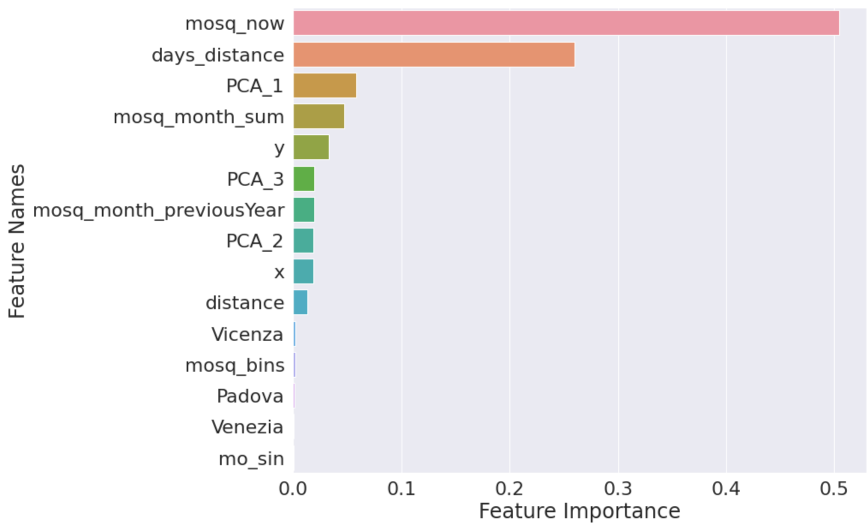

Figure 9. Feature importance of Culex Italy case without using any EO data

Other cases

MAMOTH was trained and validated with respect to its generic character and robustness in different cases of mosquito species and engaged regions (landscapes). Specifically, the model was implemented and returned high performance in (a) Serbia for the Culex pipiens (WNV), (b) Germany for the Culex pipiens (WNV), (c) Italy for the Anopheles spp. (Malaria), (d) France for the Aedes albopictus (Zika, Chikungunya, Dengue).

Figure 10 depicts the areas of interest, and Table 2 presents the main characteristics of each data collection.

Table 3 presents cumulatively the performance of MAMOTH to the aforementioned cases. The results clearly reveal that indeed the MAMOTH framework is generic and easily replicable to other cases. It is also shown that although the auto-tuned parameters are varying in the different use cases, the performance of the models remains stable and high with the maximum accuracy being returned in the case of Aedes Albopictus in France, where the MAE is surprisingly low.

Table 7 also presents the performance of MAMOTH to the aforementioned cases, but this time using only environmental data, proving the claims that the proposed framework is also applicable to regions without any previous knowledge of the current entomological situation, while Table 8 presents the performance of MAMOTH without any EO data available. Both of these tables can be found in the appendix Section.

The 13 most important features, selected by MAMOTH, and their corresponding importance for each case of interest are presented in the Table 4. Also Table 5 presents the 5 five most significant features per PCA component, so as to provide all the information needed for drawing accurate conclusions. By comparison between the different cases we can draw some insights:

- For all cases previous mosquito populations seem to play a preponderant role as is expected for the seasonal development of mosquito populations during summer months depending on the intensity of mosquito control applications in the AOI.

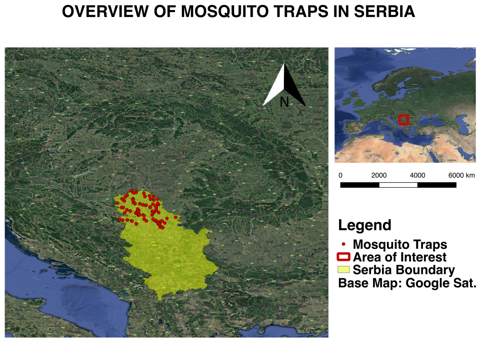

(a) Vojvodina province, Northern Serbia (Top Left 18.84, 41.85 Bottom right 23.00, 46.81 Datum WGS84).

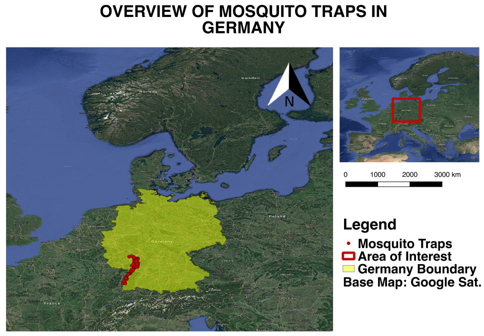

(b) Baden Wuerttemberg, Germnay (Top Left 7.58, 48.06 Bottom right 8.67, 50.03 Datum WGS84)

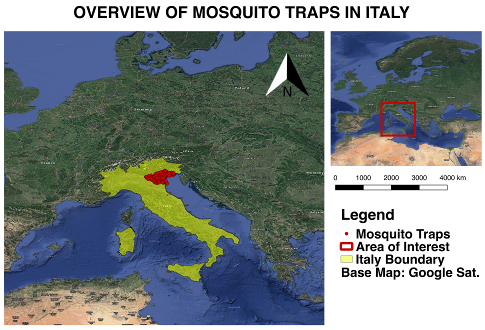

(c) Veneto region, Northeast Italy (Top Left 18.52, 46.09 Bottom right 21.47, 44.89 Datum WGS84).

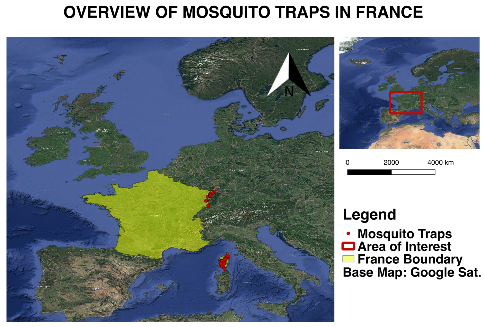

(d) Grand-Est and Corsica regions, France (Top Left 10.64, 44.90 Bottom right 13.02, 45.99 Datum WGS84).

Figure 10. The entomological networks of all cases

Table 3: MAMOTH's performance per country

Area of interest Mosquito	Auto-tuned model parameters	Performance in pre-operational validation	Performance in operational validation
Serbia Culex spp.	Nb of features = 12 Nb_estimators = 23 Max_depth = 4	MAE_test = 1.54 MAE_train = 1.27 % error < 3 = 90%	-
Germany Culex spp.	Nb of features = 33 Nb_estimators = 23 Max_depth = 4	MAE_test = 0.97 MAE_train = 0.87 % error < 3 = 92%	MAE_test = 1.19 % error < 3 = 90%
Italy Anopheles spp.	Nb of features = 47 Nb_estimators = 20 Max_depth = 8	MAE_test = 1.47 train = 1.04 % error < 3 = 95%	MAE_test = 1.60 % error < 3 = 95%
France Aedes albopictus	Nb of features = 11 Nb_estimators = 15 Max_depth = 6	MAE_test = 0.71, MAE_train = 0.63 % error < 3 = 92%	MAE_test = 1.08 % error < 3 = 95%
Italy Culex spp.	Nb of features = 16 Nb_estimators = 23 Max_depth = 5	MAE_test = 1.14, MAE_train = 1.01 % error < 3 = 97%	MAE_test = 1.27 % error < 3 = 97%

Table 4: Most important features per case

Aedes - France		Anopheles - Italy	
feature names	importance	feature names	importance
mosq_now	0.501	days_distance	0.314
lst_night	0.089	mosq_now	0.188
lst_day	0.079	DEM_1000	0.054
ndwi_mean	0.073	PCA_3	0.041
mosq_month_previousYear	0.053	Slope_1000	0.038
ndwi_std	0.043	ndwi	0.027
acc_rainfall_jan	0.042	lst_day	0.025
ndwi	0.041	ndvi_mean	0.024
PCA_2	0.029	celsius	0.024
PCA_3	0.027	ndvi_std	0.021
mo_cos	0.023	y	0.020
		LST_jan_mean	0.017
		mosq_month_sum	0.014
Culex - Serbia		**Culex - Germany**	
feature names	importance	feature names	importance
mosq_month_sum	0.265	mosq_now	0.675
days_distance	0.257	days_distance	0.095
mosq_now	0.187	mosq_bins	0.049
acc_rainfall_jan	0.083	acc_rainfall_2week2	0.039
LST_Mar_mean	0.039	acc_rainfall_jan	0.027
DEM_1000	0.036	acc_rainfall_1week	0.022
acc_rainfall_2week2	0.036	mo_cos	0.014
Slope_1000	0.027	LST_Apr_mean	0.014
max_wind	0.022	ndwi_mean	0.011
mosq_month_previousYear	0.021	LST_Jan_mean	0.005
PCA_2	0.016	x	0.005
celsious	0.011	Aspect_1000	0.004
		mosq_month_sum	0.004

- The accumulated rainfall from the beginning of the year is important for all the cases, and for the cases of Culex spp., the accumulated rainfall of the last two weeks seems important as well.
- In all Culex spp. cases, the rainfall and the water indices, NDWI, are more important than the temperature, LST
- Anopheles is the only mosquito genus in which the most important feature is not the previous state of the mosquito population but the direct time distance as well as several geomorphological features which could indicate the preference of mosquitoes of this genus of stagnant water surfaces in specific altitudes.
- Aedes albopictus prediction is the only case were the direct time distance is not important for the model. Furthermore, the Aedes albopictus populations seem to be very sensible to temperature, more than to precipitation, while both are important factors for the creation and durability of breeding sites for this container breeding species.
- NDWI metrics are very important for the prediction of Aedes albopictus populations compared with the other mosquito species.

Tables 9 and 10 that present the most significant feature per case using only EO data and without using any EO data respectively can be found in the appendix Section.

5. Discussion / Conclusions

In this paper we saw that it is feasible to develop a generic machine learning model that predicts mosquito populations without any special design regarding the area of interest or the mosquito species. We prove that this approach achieves accurate and reliable performance, by relying on common satellite and entomological data. Additionally,

Table 5: PCA features most significant components per case using both EO and entomological data

Area of interest Mosquito	PCA_1	PCA_2	PCA_3
Italy Culex spp	W_area_1km	Flow_acc_1000	Coast_dist_1000
	Coast_dist_1000	W_area_1km	W_area_1km
	Flow_acc_1000	Coast_dist_1000	lst_night
	WC_L_1km	lst_night	Flow_acc_1000
	WC_dist_1000	WC_L_1km	WC_L_1km
Serbua Culex spp	PG_area_1km	Coast_dist_1000	Flow_acc_1000
	Flow_acc_1000	lst_night	WC_dist_1000
	Coast_dist_1000	mosq_month_previousYear	WC_L_1km
	WC_L_1km	WC_dist_1000	mosq_month_sum
	lst_night	PG_area_1km	mosq_now
Germany Culex spp	Flow_acc_1000	mosq_month_sum	lst_day
	LST_Mar_mean	mosq_now	lst_night
	lst_day	lst_night	LST_Apr_mean
	LST_Feb_mean	acc_rainfall_jan	mosq_month_sum
	LST_Apr_mean	lst_day	LST_Mar_mean
Italy Anopheles spp.	W_area_1km	Flow_acc_1000	Coast_dist_1000
	Coast_dist_1000	Coast_dist_1000	W_area_1km
	Flow_acc_1000	W_area_1km	Flow_acc_1000
	WC_L_1km	WC_L_1km	WC_L_1km
	mosq_month_sum	WC_dist_1000	WC_dist_1000
France Aedes Albopictus	Coast_dist_1000	PG_area_1km	Flow_acc_1000
	PG_area_1km	Flow_acc_1000	PG_area_1km
	WC_L_1000	Coast_dist_1000	WC_L_1km
	Flow_acc_1000	WC_L_1km	LST_Jan_mean
	lst_day	DEM_1000	Coast_dist_1000

this direction gives us the opportunity of comparative study between different areas or mosquitoes.

The results show that indeed the model manages to be auto-calibrated for the different cases by selecting different features and parameters. Additionally, our approach offered the capability of comparative studies and the extraction of valuable information, which without that generic and unified approach could not have been possible.

Furthermore, the results of MAMOTH for predictions away of the trap-site, if the model is trained only upon environmental and not past entomological data, were promising, as the performance did not deviate much from the initial model. Thus, even in lack of entomological data, the system remains robust and able to predict mosquito populations. This variation of the system offers a more flexible model applicable even to communities that do not have dense entomological networks, once the model can extrapolate the mosquitoes abundance between the traps. However the use of entomological data offers valuable information to the model enabling for more accurate predictions. An important difference between the two models, however, is the number of features selected by the model. In the second case where only EO data are used, the number of features is significantly larger. This direction of research is quite promising once the off-trap site prediction increases massively the applications of the model.

Acknowledgments

MAMOTH was developed in the framework of the EYWA project, an EarlY WArning System for Mosquito-Borne Diseases, an initiative under the flag of the EuroGEO Action Group “EO4EViDence - Earth Observation for Epidemics of Vector-Borne Diseases". We would like to specially thank our partners for their entomological data contribution, namely the Istituto Zooprofilattico Sperimentale delle Venezie, and the Veneto and Friuli-Venezia Giulia Regions for Italy’s data; the Faculty of Agriculture in the University of Novi Sad for Serbia's data; the Kommunale Aktionsgemeinschaft zur Bekämpfung der Schnakenplage e.V. for Germany's data; and the Entente Interdépartementale pour la démoustication du littoral Méditerranéen for France's data.

References

1. World Health Organization. Vector-borne diseases. 2020. Available online: https://www.who.int/en/news-room/fact-sheets/detail/vector-borne-diseases (accessed on 30 December 2020).
2. Parselia, E.; Kontoes, C.; Tsouni, A.; Hadjichristodoulou, C.; Kioutsioukis, I.; Magiorkinis, G.; Stilianakis, N.I. Satellite Earth Observation Data in Epidemiological Modeling of Malaria, Dengue and West Nile Virus: A Scoping Review.*Remote Sens* **2019**, *11*, 1862 [Google Scholar]
3. Zeller, H.; Marrama, L.; Sudre, B.; Van Bortel, W.; Warns-Petita, E. Mosquito-borne disease surveillance by the European Centre for Disease Prevention and Control. *European Society of Clinical Microbiology and Infectious Diseases* **2013**, *19(8)*, 693–698. [Google Scholar]
4. Paz, S.; Semenza, J.C. Environmental Drivers of West Nile Fever Epidemiology in Europe and Western Asia—A Review. 10, 3543-3562. https://doi.org/10.3390/ijerph10083543*Int. J. Environ. Res. Public Health* **2013**, *10*, 3543-3562. [Google Scholar]
5. ECDC. West Nile virus infection - Annual Epidemiological Report for 2018. Available online: https://www.ecdc.europa.eu/en/publications-data/west-nile-virus-infection-annual-epidemiological-report-2018 (accessed on 25 November 2020).
6. ECDC. Malaria - Number and rates of confirmed malaria reported cases, EU/EEA 2008–2012. Available online: https://www.ecdc.europa.eu/en/publications-data/number-and-rates-confirmed-malaria-reported-cases-eueea-2008-2012 (accessed on 25 November 2020).
7. ECDC. Malaria - Annual Epidemiological Report for 2018. Available online: https://www.ecdc.europa.eu/en/publications-data/malaria-annual-epidemiological-report-2018 (accessed on 25 November 2020).
8. Guo, S.; Ling, F.; Hou, J.; Wang, J.; Fu, G.; Gong, Z. Mosquito Surveillance Revealed Lagged Effects of Mosquito Abundance on Mosquito-Borne Disease Transmission: A Retrospective Study in Zhejiang, China. *PLOS ONE* **2014**, *9(11)*. [Google Scholar]
9. Kotchi, SO; Bouchard, C.; Ludwig, A.; Rees, EE; Brazeau, S. Using Earth observation images to inform risk assessment and mapping of climate change-related infectious diseases. *Can Commun Dis Rep* **2019**, *45(5)*, 133-142. [Google Scholar]
10. Guo, H.; Nativi, S.; Liang, D.; Craglia, M.; Wang, L.; Schade, S.; Corban, C.; He, G.; Pesaresi, M.; Li, J.; Shirazi, Z.; Liu, J.; Annoni,A. Big Earth Data science: an information framework for a sustainable planet. *International Journal of Digital Earth* **2020**, *13(7)*, 743-767. [Google Scholar]
11. Kioutsioukis, I; Stilianakis, N.I. Assessment of West Nile virus transmission risk from a weather-dependent epidemiological model and a global sensitivity analysis framework. *Acta Tropica* **2019**, *193*, 129-141. [Google Scholar]
12. Jutla, A.; Huq, A.; Colwell, RR. A Diagnostic approach for monitoring hydroclimatic conditions related to emergence of west nile virus in west virginia. *Front Public Health* **2015**, *3*, 10. [Google Scholar]
13. Valiakos, G.; Papaspyropoulos, K.; Giannakopoulos, A.; Birtsas, P.; Tsiodras, S.; Hutchings, MR; Spyrou, V.; Pervanidou, D.; Athanasiou, LV; Papadopoulos, N.; Tsokana, C.; Baka, A.; Manolakou, K.; Chatzopoulos, D.; Artois, M.; Yon, L.; Hannant, D.; Petrovska, L.; Hadjichristodoulou, C.; Billinis, C. Use of wild bird surveillance, human case data and GIS spatial analysis for predicting spatial distributions of West Nile virus in Greece. *PLoS One* **2014**, *9(5)* [Google Scholar]
14. Calistri, P.; Ippoliti, C.; Candeloro, L.; Benjelloun, A.; El Harrak, M.; Bouchra, B.; Danzetta, ML; Di Sabatino, D.; Conte, A. Analysis of climatic and environmental variables associated with the occurrence of West Nile virus in Morocco. *rev Vet Med* **2013**, *110(3-4)*, 549-553. [Google Scholar]
15. Yao, J; Meng, D; Zhao, Q; Cao, W; Xu, Z. Nonconvex-Sparsity and Nonlocal-Smoothness-Based Blind Hyperspectral Unmixing, *IEEE Transactions on Image Processing* **2019**, *28(6)*, 2991-3006. [Google Scholar]
16. Gao, L; Yokoya, N; Yao, J; Chanussot, J; Du, Q. More Diverse Means Better: Multimodal Deep Learning Meets Remote-Sensing Imagery Classification. *IEEE Transactions on Geoscience and Remote Sensing* **2020**, *PP*, 1-15. [Google Scholar]

17. Lary D.; Alavi A.; Gandomi A.; Walker A. Machine learning in geosciences and remote sensing, *Geoscience Frontiers* **2016**, *7(1)*, 3-10. [Google Scholar]
18. Sudheer, Ch; Sohani, S. K.; Kumar, D.; Malik, A.; Chahar, B. R.; Nema, A. K.; Panigrahi, B. K.; Dhiman, R. C. 2014. A Support Vector Machine-Firefly Algorithm based forecasting model to determine malaria transmission. *Neurocomputing* **2014**, *129*, 279–288. [Google Scholar]
19. Guo, P.; Liu, T.; Zhang, Q.; Wang, L.; Xiao, J.; Zhang, Q.; Luo, G.; Li, Z.; He, J.; Zhang, Y.; Ma, W. Developing a dengue forecast model using machine learning: A case study in China. *PLoS Negl Trop Dis* **2017**, *11(10)*. [Google Scholar]
20. Chuang, TW; Wimberly, MC; Remote sensing of climatic anomalies and West Nile virus incidence in the northern Great Plains of the United States. *PLoS One* **2012**, *7(10)*. [Google Scholar]
21. Sewe, M. O.; Tozan, Y.; Ahlm, C.; Rocklöv, J. Using remote sensing environmental data to forecast malaria incidence at a rural district hospital in Western Kenya. *Scientific reports* **2017**, *7(1)*, 2589. [Google Scholar]
22. Scavuzzo, J.M.; Trucco, F.; Espinosa, M.; Tauro, C.B.; Abril, M.; Scavuzzo, C.M.; Frery, A.C. Modeling Dengue vector population using remotely sensed data and machine learning. *Acta Tropica* **2018**, *185*, 167-175. [Google Scholar]
23. Young, S. G; Tullis, J. A; Cothren, J. A remote sensing and GIS-assisted landscape epidemiology approach to West Nile virus. *Applied geography* **2013**, *45*, 241-249. [Google Scholar]
24. Dohm, D.J.; O'Guinn, M.L.; Turell, M.J. Effect of environmental temperature on the ability of Culex pipiens (Diptera: Culicidae) to transmit West Nile virus. *J Med Entomol.* **2002**, *39(1)*, 221-225. [Google Scholar]
25. Myer, M. H; Johnston, J. M. Spatiotemporal Bayesian modeling of West Nile virus: Identifying risk of infection in mosquitoes with local-scale predictors. *The Science of the total environment* **2019**, *650(2)*, 2818-2829. [Google Scholar]
26. Stilianakis, N. I.; Syrris, V.; Petroliagkis, T.; Pärt, P.; Gewehr, S.; Kalaitzopoulou, S.; Mourelatos, S.; Baka, A.; Pervanidou, D.; Vontas, J.; Hadjichristodoulou, C. Identification of Climatic Factors Affecting the Epidemiology of Human West Nile Virus Infections in Northern Greece. *PloS one* **2016**, *11(9)*. [Google Scholar]
27. Chuang, T.-W.; Hildreth, B. M.; Vanroekel, L. D.; Wimberly, C. M. Weather and Land Cover Influences on Mosquito Populations in Sioux Falls, South Dakota. *Journal of Medical Entomology* **2011**, *48(3)*, 669–679. [Google Scholar]
28. Richman, M; Trafalis, T; Adrianto, I. Missing Data Imputation Through Machine Learning Algorithms. *Artificial Intelligence Methods in the Environmental Sciences* **2009**, 153–169. [Google Scholar]
29. Friedman, J. Greedy function approximation: a gradient boosting machine. *Annals of Statistics* **2001**, *29(5)*, 1189–1232. [Google Scholar]
30. Hastie, T.; Tibshirani, R.; Friedman, J. The Elements of Statistical Learning. *Springer New York Inc.* **2001**, 367. [Google Scholar]
31. Witten I.;and Frank E.; Hall M.; Pal C. Chapter 6 - Trees and rules. *Data Mining (Fourth Edition)* **2017**, 209-242. [Google Scholar]

705 **Appendix**

Table 6: Feature List

Feature	Explanation
dt_placeme	Date of the observation
stationid	Station ID
x	Longitude
y	Latitude
mosq_now	Mosquito population in trapping sites at the date of observation
NDVI	Proxy for the vegetation density and distribution. Extracted pixel value of overlapping station ID coordinates
NDVI_mean	Proxy for the vegetation density and distribution. Mean value of neighboring pixels (window of 3x3)
NDVI_std	Proxy for the vegetation density and distribution. Standard deviation of neighboring pixels (window of 3x3)
NDWI	Proxy for changes in water content Extracted pixel value of overlapping station ID coordinates
NDWI_mean	Proxy for changes in water content Mean value of neighboring pixels (window of 3x3)
NDWI_std	Proxy for changes in water content Standard deviation of neighboring pixels (window of 3x3)
NDMI	Proxy for determination of vegetation water content Extracted pixel value of overlapping station ID coordinates
NDMI_mean	Proxy for determination of vegetation water content Mean value of neighboring pixels (window of 3x3)
NDMI_std	Proxy for determination of vegetation water content Standard deviation of neighboring pixels (window of 3x3)
NDBI	Proxy for mapping urban built-up areas Extracted pixel value of overlapping station ID coordinates
NDBI_mean	Proxy for mapping urban built-up areas Mean value of neighboring pixels (window of 3x3)
NDBI_std	Proxy for mapping urban built-up areas Standard deviation of neighboring pixels (window of 3x3)
LST_day	Land surface temperature at day
LST_night	Land surface temperature at night
LST_Jan_mean	Mean temperature in January
LST_Feb_mean	Mean temperature in February
LST_Mar_mean	Mean temperature in March
LST_Apr_mean	Mean temperature in April
wind_max	Max magnitude of wind
wind_mean	Mean magnitude of wind hourly
wind_min	Min magnitude of wind
acc_rainfall_1week	Accumulated precipitation counting towards one week before the date of placement
acc_rainfall_2week2	Accumulated precipitation counting towards two weeks before the date of placement
acc_rainfall_jan	Accumulated precipitation counting from the 1st of January of each year
WC_L_1km	Combination of breeding site length and water course of national hydrological data within a buffer zone of 1000 m around each sampling/trapping site
PG_area_1km	Total area of temporarily inundated areas (polygons) within a buffer zone of 1km from each sampling/trapping site

Feature	Explanation
DEM_1000	Mean elevation (resolution = 12.5 m), within a buffer of 1000m around trapping sites
Aspect_1000	Mean aspect (12.5 m), within a buffer of 1000 m around trapping sites
Slope_1000	Mean slope (12.5 m), within a buffer of 1000 m around trapping sites
Coast_dist_1000	Mean Distance of sampling/trapping site within a buffer of 1000m from coastline
WC_dist_1000	Distance of combination of breeding site length and length of watercourses of national hydrological data within a buffer zone of 1000m around each sampling/trapping site
Flow_acc_1000	Mean flow accumulation within a buffer of 1000 around trapping sites
mosq_month_sum	Cumulative mosquito population of the past 30 days
mosq_month_previousYear	Cumulative mosquito population of the month on previous year
mosq_bins	Mosquito bin based on the population on the date of observation
days_distance	Time difference in days between the date of placement and a specific date regardless the year
province (multiple features)	Province in which trap is located (transformed in one hot encoded features out of the names of the provinces of each region)
mo_cos	Cosine transformation of the month of date of placement
mo_sin	Sine transformation of the month of date of placement
celsius	LST_day to celsius conversion
summer_days_year	Days with over 30^o celsius within the year
summer_days_month	Days with over 30^o celsius within the month
PCA components	3 PCA components extracted from the whole dataset
distance	Euclidean distance of coordinates between a specific point and the trap site

Table 7: MAMOTH's pre-operational applications and performance per country using only EO data

Area of interest Mosquito	Auto-tuned model parameters	MAE in Nb classes	Prediction < 3 classes error
Serbia Culex spp.	Nb of features = 37 Nb_estimators = 11 Max_depth = 14	test=1.88, train=0.81	87%
Germany Culex spp.	Nb of features = 22 Nb_estimators = 31 Max_depth = 4	test=1.18, train=1.07	89%
Italy Anopheles spp.	Nb of features = 51 Nb_estimators = 33 Max_depth = 6	test=1.48, train=0.54	94%
France Aedes albopictus	Nb of features = 42 Nb_estimators = 20 Max_depth = 14	test=0.72, train=0.96	87%
Italy Culex spp.	Nb of features = 34 Nb_estimators = 27 Max_depth = 9	test=1.20, train=0.60	96%

Table 8: MAMOTH's pre-operational applications and performance per country without using any EO features

Area of interest Mosquito	Auto-tuned model parameters	MAE in Nb classes	Prediction < 3 classes error
Serbia Culex spp.	Nb of features = 3 Nb_estimators = 20 Max_depth = 7	test=1.73, train=1.18	86%
Germany Culex spp.	Nb of features = 4 Nb_estimators = 28 Max_depth = 4	test=1.04, train=0.99	90%
Italy Anopheles spp.	Nb of features = 20 Nb_estimators = 26 Max_depth = 9	test=1.54 train=0.27	92%
France Aedes albopictus	Nb of features = 13 Nb_estimators = 26 Max_depth = 3	test=0.74, train=0.63	91%
Italy Culex spp.	Nb of features = 15 Nb_estimators = 24 Max_depth = 8	test=1.16, train=0.76	95%

Table 9: Most important features per case without using EO data

Aedes-France		Anopheles-Italy	
feature names	importance	feature names	importance
mosq_now	0.561	days_distance	0.303
days_disance	0.200	mosq_now	0.209
PCA_3	0.049	distance	0.077
mosq_monh_sum	0.040	mosq_monh_sum	0.077
PCA_1	0.035	mosq_monh_previousYear	0.072
PCA_2	0.031	PCA_3	0.071
x	0.026	PCA_1	0.067
y	0.022	PCA_2	0.063
mo_sin	0.017	Treviso	0.012
mosq_month_previousYear	0.015	Padova	0.010
distance	0.004	Rovigo	0.009
HAUE-CORSE	0.000	mosq_bins	0.009
mosq_bins	0.000	Venezia	0.008
		Vicenza	0.004
		mo_sin	0.002
		Verona	0.002
		Gorizia	0.002
		mo_cos	0.002
		Pordenone	0.001
		Udine	0.000
Culex-Serbia		**Culex-Germany**	
feature names	importance	feature names	importance
PCA_1	0.397	mosq_now	0.592
days_distance	0.388	mosq_bins	0.223
mosq_monh_previousYear	0.215	mo_cos	0.105
		PCA_3	0.079

Table 10: Most important features per case using only EO data

Aedes-France		Anopheles-Italy	
feature_names	importance	feature_names	importance
x	0.150	days_distance	0.274
lst_night	0.137	DEM_1000	0.082
PCA_2	0.059	PCA_3	0.049
ndwi	0.055	ndwi	0.041
ndvi	0.039	Slope_1000	0.039
acc_rainfall_2week2	0.038	LST_Jan_mean	0.038
ndvi_std	0.038	PCA_2	0.038
days_distance	0.035	ndwi_std	0.033
ndwi_mean	0.034	ndvi_std	0.032
PCA_1	0.033	ndvi_mean	0.026
ndmi	0.031	lst_night	0.023
ndbi_mean	0.030	acc_rainfall_jan	0.023
PCA_3	0.028	ndwi_mean	0.023
acc_rainfall_jan	0.026	celsius	0.021
ndvi_mean	0.024	lst_day	0.021
summer_days_month	0.024	acc_rainfall_2week2	0.019
ndwi_std	0.022	acc_rainfall_1week	0.016
acc_rainfall_1week	0.021	y	0.015
ndmi_mean	0.021	ndmi	0.014
distance	0.020	ndvi	0.014
Culex-Serbia		Culex-Germany	
feature_names	importance	feature_names	importance
days_distance	0.118	acc_rainfall_jan	0.343
acc_rainfall_1week	0.076	days_distance	0.158
mean_wind	0.071	y	0.155
acc_rainfall_jan	0.063	distance	0.058
PCA_3	0.037	acc_rainfall_2week2	0.054
y	0.035	mo_cos	0.025
PCA_2	0.034	x	0.023
DEM_1000	0.034	ndmi_mean	0.023
lst_night	0.029	WAW	0.020
PCA_1	0.027	lst_night	0.017
Aspect_1000	0.027	acc_rainfall_1week	0.015
ndwi_std	0.027	ndvi_std	0.014
max_wind	0.025	ndmi	0.013
ndvi_mean	0.024	DEM_1000	0.011
LST_Jan_mean	0.023	LST_Apr_mean	0.011
acc_rainfall_2week2	0.022	LST_Jan_mean	0.011
Slope_1000	0.020	PCA_3	0.011
ndwi	0.020	ndwi	0.009
Sremski	0.018	ndwi_mean	0.009
LST_Feb_mean	0.018	celsius	0.007